

Neutral Higgs-pair Production at one-loop from a Generic 2HDM

David López-Val*

*High Energy Physics Group, Dept. ECM and Institut de Ciències del Cosmos
Universitat de Barcelona
Av. Diagonal 647, E-08028 Barcelona, Catalonia, Spain
E-mail: dlopez@ecm.ub.es*

Joan Solà

*High Energy Physics Group, Dept. ECM and Institut de Ciències del Cosmos
Universitat de Barcelona
Av. Diagonal 647, E-08028 Barcelona, Catalonia, Spain
E-mail: sola@ecm.ub.es*

We present a one-loop analysis of the pairwise production of neutral Higgs bosons (h^0A^0, H^0A^0) at linear colliders, such as the ILC and CLIC, within the general Two-Higgs-Doublet Model (2HDM). We single out sizable radiative corrections, which can well reach the level of $|\delta\sigma|/\sigma \sim 50\%$ and may be either positive (typically for $\sqrt{s} \simeq 0.5$ TeV) and negative (for $\sqrt{s} \gtrsim 1$ TeV). These large quantum effects, obtained in full agreement with the current phenomenological bounds and the stringent theoretical constraints on the parameter space of the model, can be traced back to the enhancement capabilities of the triple-Higgs self-interactions – a trademark feature of the 2HDM, with no counterpart in e.g. the Minimal Supersymmetric Standard Model. In the most favorable scenarios, the Higgs-pair cross sections may be boosted up to barely 30 fb at the fiducial center-of-mass energy of 500 GeV – amounting to $\mathcal{O}(\sim 10^3)$ events per 500 fb^{-1} of integrated luminosity. We also compare these results with several complementary double and triple Higgs-boson production mechanisms at order $\mathcal{O}(\alpha_{ew}^3)$ and leading $\mathcal{O}(\alpha_{ew}^4)$, and we spotlight a plethora of potentially distinctive signatures of a Two-Higgs-Doublet structure of non-supersymmetric nature.

*RADCOR 2009 - 9th International Symposium on Radiative Corrections (Applications of Quantum Field Theory to Phenomenology)
October 25-30 2009
Ascona, Switzerland*

*Speaker.

1. Introduction

The Two-Higgs-Doublet Model (2HDM) is a particularly simple extension of the Standard Model (SM) which already encompasses outstanding new phenomenology [1]. In addition, a Two-Higgs-Doublet structure naturally emerges as the low-energy realization of some more fundamental theories – viz. the Higgs sector of the Minimal Supersymmetric Standard Model (MSSM) [2]. The 2HDM spectrum contains two neutral CP -even (h^0, H^0), one CP -odd (A^0) and two charged Higgs bosons (H^\pm) and, as a most distinctive feature, it allows triple (3H) and quartic (4H) Higgs self-interactions to be largely enhanced – in contrast to the MSSM, wherein such couplings are restrained by the gauge symmetry. The phenomenological impact of such potentially large 3H self-interactions has been actively investigated at linear colliders within a manifold of processes, to wit: the tree-level production of triple Higgs-boson final states [3]; the double Higgs-strahlung channels hhZ^0 [4]; and the inclusive Higgs-pair production via gauge-boson fusion [5]. Likewise, the $\gamma\gamma$ mode of linac facilities has also been considered, in particular within the loop-induced single [6] and double Higgs production processes [7]. All these mechanisms would be capable to yield large Higgs production rates and furnish experimental signatures which, owing to the clean environment inherent to linear colliders, might enable for precise measurements of e.g. the Higgs boson masses, their couplings to fermions and gauge bosons and their own self-interactions; this means, to reconstruct the Higgs potential itself. Moreover, these large rates could be also revealing by themselves, as they could not be deemed e.g. to a SUSY origin due to the intrinsically different nature of Higgs self-interactions.

Similarly, double Higgs boson (2H) production may be also instrumental at future linac facilities [8]. Such processes cannot proceed at the tree-level in the SM, which means that, if we would detect a sizable rate of 2H final states e.g. of the sort $e^+e^- \rightarrow h^0A^0; H^0A^0; H^+H^-$, this would entail an unmistakable sign of new physics. Nonetheless, a tree-level analysis of these processes is most likely insufficient to disentangle e.g. SUSY and non-SUSY extensions of the Higgs sector, as the tree-level hA^0Z^0 couplings ($h = h^0, H^0$) are purely gauge, and hence both models can give rise to similar cross-sections at the leading-order. One-loop corrections to these 2H production rates are therefore required to this effect. A number of studies are available within the MSSM [9] whilst, on the 2HDM side, the efforts were first concentrated on the production of charged Higgs pairs [10] and, only very recently, they have been extended to the neutral sector [11].

2. Computation setup

The general 2HDM [1] is obtained upon canonical extension of the SM Higgs sector with a second $SU_L(2)$ doublet with weak hypercharge $Y = +1$. The seven free parameters λ_i in the general, CP -conserving, 2HDM can be sorted out as follows: the masses of the physical Higgs particles ($M_{h^0}, M_{H^0}, M_{A^0}, M_{H^\pm}$), $\tan\beta$ (the ratio of the two VEV's $\langle H_i^0 \rangle$), the mixing angle α between the two CP -even states; and one Higgs self-coupling λ_5 . Additionally, the Higgs couplings to fermions must be engineered so that no tree-level flavor changing neutral currents (FCNC) are allowed: this gives rise to the following basic scenarios, namely Types-I and II 2HDM – see [1] for details. Further constraints must be imposed to assess that the SM behavior is sufficiently well reproduced up to the energies explored so far, namely: *i*) the perturbativity and unitarity bounds [12]; *ii*)

the approximate $SU(2)$ custodial symmetry, which requires $|\delta\rho_{2HDM}| \lesssim 10^{-3}$ [13]; and *iii*) the consistency with the low-energy radiative B -meson decays (which demands $M_{H^\pm} \gtrsim 300$ GeV for $\tan\beta \geq 1$ in the case of type-II 2HDM [14]). We refer the reader to [11] for further details on the model setup and the constraints.

Hereafter, our endeavor will be basically threefold: i) to single out the regions in the 2HDM parameter space for which the $e^+e^- \rightarrow A^0h^0/A^0H^0$ production is optimized; ii) to quantify the numerical impact of the associated quantum effects; and iii) to correlate the latter with the enhancement capabilities of 3H self-interactions. For definiteness, let us concentrate on the h^0A^0 channel. Our starting point shall be the $e^+e^- \rightarrow h^0A^0$ scattering amplitude at 1-loop,

$$\mathcal{M}_{e^+e^- \rightarrow A^0h^0} = \sqrt{\hat{Z}_{h^0}} \mathcal{M}_{e^+e^- \rightarrow A^0h^0}^{(0)} + \mathcal{M}_{e^+e^- \rightarrow A^0h^0}^{(1)} + \delta \mathcal{M}_{e^+e^- \rightarrow A^0h^0}^{(1)},$$

where $\sqrt{\hat{Z}_{h^0}}$ stands for the finite WF renormalization of the external h^0 leg, which we shall expand as $\sqrt{\hat{Z}_{h^0}} = 1 - \frac{1}{2} \text{Re} \hat{\Sigma}'_{h^0h^0}(M_{h^0}^2)$, in order to retain only those contributions which are at leading-order in the triple-Higgs self-couplings. In turn, $\mathcal{M}_{e^+e^- \rightarrow A^0h^0}^{(1)}$ includes the entire set of $\mathcal{O}(\alpha_{ew}^2, \alpha_{ew} \alpha_{em})$ one-loop contributions, to wit: i) the vacuum polarization corrections to the Z^0 -boson propagator and the $Z^0 - \gamma$ mixing; ii) the loop-induced γA^0h^0 interaction; iii) the vertex corrections to the $e^+e^-Z^0$ and $h^0A^0Z^0$ interactions; and iv) box-type contributions. Finally, the 1-loop counterterm $\delta \mathcal{M}_{e^+e^- \rightarrow A^0h^0}^{(1)}$ guarantees that the overall amplitude \mathcal{M} is UV-finite. Such counterterm ought to be anchored by a set of renormalization conditions; for the SM fields and parameters, we stick to the conventional on-shell scheme in the Feynman gauge, see e.g. [15]. Concerning the renormalization of the 2HDM Higgs sector, we also employ an on-shell scheme whose implementation is discussed in full detail in [11].

3. Numerical results

The basic quantities of interest are: i) the predicted cross section at the Born-level $\sigma^{(0)}$ and at 1-loop $\sigma^{(0+1)}$, in which we include the full set of $\mathcal{O}(\alpha_{ew}^3)$ corrections, and also the leading $\mathcal{O}(\alpha_{ew}^4)$ which come from the squared of the scattering amplitude \mathcal{M} ; and ii) the relative size of the 1-loop radiative corrections, which we track through the parameter $\delta_r = \frac{\sigma^{(0+1)} - \sigma^{(0)}}{\sigma^{(0)}}$. Throughout the present work we make use of the standard computational packages [16]. For definiteness, we sort out the Higgs boson masses as follows:

	M_{h^0} [GeV]	M_{H^0} [GeV]	M_{A^0} [GeV]	M_{H^\pm} [GeV]
Set A	130	150	200	160
Set B	150	200	260	300

We shall use type-I 2HDM for Set A, and type-II for Set B – as, in the latter case, M_{H^\pm} is suitable to elude $\mathcal{B}(b \rightarrow s\gamma)$ constraints. The predictions for both sets are quoted in Table 1 for different values of the hA^0Z^0 tree-level coupling and maximally enhanced 3H self interactions – namely $\tan\beta = 1$ and $\lambda_5 \simeq -10$ (resp. -8) for Set A (resp. Set B).

These results single out large quantum effects ($|\delta\sigma|/\sigma \sim 20 - 60\%$), which can be either positive (for $\sqrt{s} \simeq 0.5$ TeV) or negative ($\sqrt{s} \gtrsim 1$ TeV) and turn out to be fairly independent on the

$\sqrt{s} = 0.5 \text{ TeV}$		$h^0 A^0$			$H^0 A^0$		
		$\alpha = \beta$	$\alpha = \beta - \pi/6$	$\alpha = \pi/2$	$\alpha = \beta - \pi/2$	$\alpha = \beta - \pi/3$	$\alpha = 0$
Set A	$\sigma_{max} [\text{fb}]$	26.71	20.05	13.10	26.32	17.53	10.29
	$\delta_r [\%]$	31.32	31.42	28.81	48.45	31.82	16.10
Set B	$\sigma_{max} [\text{fb}]$	11.63	9.08	6.36	5.00	3.28	1.95
	$\delta_r [\%]$	35.17	40.68	47.86	71.81	50.22	34.15

$\sqrt{s} = 1 \text{ TeV}$		$h^0 A^0$			$H^0 A^0$		
		$\alpha = \beta$	$\alpha = \beta - \pi/6$	$\alpha = \pi/2$	$\alpha = \beta - \pi/2$	$\alpha = \beta - \pi/3$	$\alpha = 0$
Set A	$\sigma_{max} [\text{fb}]$	4.08	2.70	1.56	3.59	2.52	1.55
	$\delta_r [\%]$	-58.42	-63.28	-68.11	-62.62	-65.09	-67.75
Set B	$\sigma_{max} [\text{fb}]$	6.11	4.22	2.86	5.17	3.98	2.75
	$\delta_r [\%]$	-30.16	-35.62	-34.58	-36.80	-35.14	-32.80

Table 1: Maximum total cross section $\sigma^{(0+1)}(e^+e^- \rightarrow A^0 h^0)$ and relative radiative correction (δ_r) at $\sqrt{s} = 0.5 \text{ TeV}$ and $\sqrt{s} = 1 \text{ TeV}$, for Sets A and B of Higgs masses. The results are obtained at fixed $\tan \beta = 1$ and different values of α , with $\lambda_5 \simeq -10$ (resp. -8) for Set A (resp. Set B).

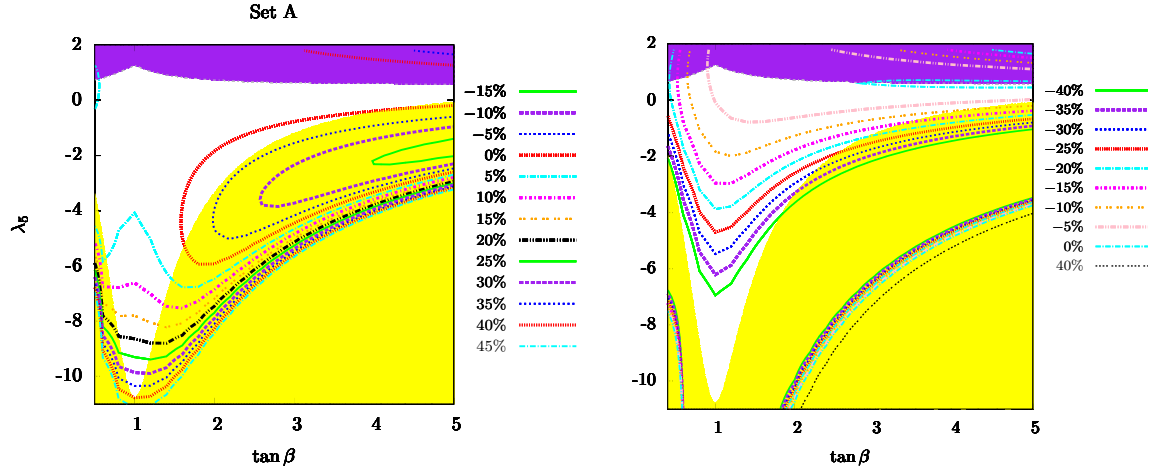


Figure 1: Contour plots of the quantum corrections δ_r (in %) to the $e^+e^- \rightarrow A^0 h^0$ cross-section as a function of $\tan \beta$ and λ_5 , for Set A of Higgs boson masses, $\alpha = \beta$ and $\sqrt{s} = 0.5 \text{ TeV}$ (left panel), $\sqrt{s} = 1.0 \text{ TeV}$ (right panel). The shaded areas are excluded by the vacuum stability (top purple area) and the unitarity bounds (bottom yellow area).

details of the Higgs mass spectrum, the particular type of 2HDM and the specific channel under analysis ($h^0 A^0, H^0 A^0$). The corresponding cross-sections at 1-loop lie in the approximate range of $2 - 30 \text{ fb}$ for $\sqrt{s} = 0.5 \text{ TeV}$ – up to barely $10^3 - 10^4$ events per 500 fb^{-1} . As for the radiative corrections themselves, in Figure 1 we display their detailed behavior (for $h^0 A^0$) as a function of $\tan \beta$ and λ_5 , as well as their interplay with the unitarity bounds (lower area, in yellow) and the vacuum stability conditions (upper area, in purple). Notice that the former disallows simultaneously large values of $\tan \beta$ and λ_5 , whereas the latter enforces $\lambda_5 \lesssim 0$. The largest attainable quantum effects (positive or negative, depending on \sqrt{s}) are identified in a valley-shaped region at $\tan \beta \simeq 1$ and $|\lambda_5| \sim 5 - 10$. In such regimes, a subset of 3H self-couplings becomes substantially augmented – their strength growing with $\sim |\lambda_5|$ – and stand as a preminent source of radiative corrections – via Higgs-boson mediated 1-loop corrections to the $h A^0 Z^0$ vertex. As a result the latter interaction,

which is purely gauge at the tree-level, becomes drastically promoted at the 1-loop order. Upon simple power counting arguments and educated guess we may barely estimate the loop-corrected $h^0 A^0 Z^0$ coupling as $\Gamma_{h^0 A^0 Z^0}^{eff} \sim \Gamma_{h^0 A^0 Z^0}^0 \lambda_{3H}^2 / 16\pi^2 s \times f(M_{h^0}^2/s, M_{A^0}^2/s)$, where $f(M_{h^0}^2/s, M_{A^0}^2/s)$ is a dimensionless form factor.

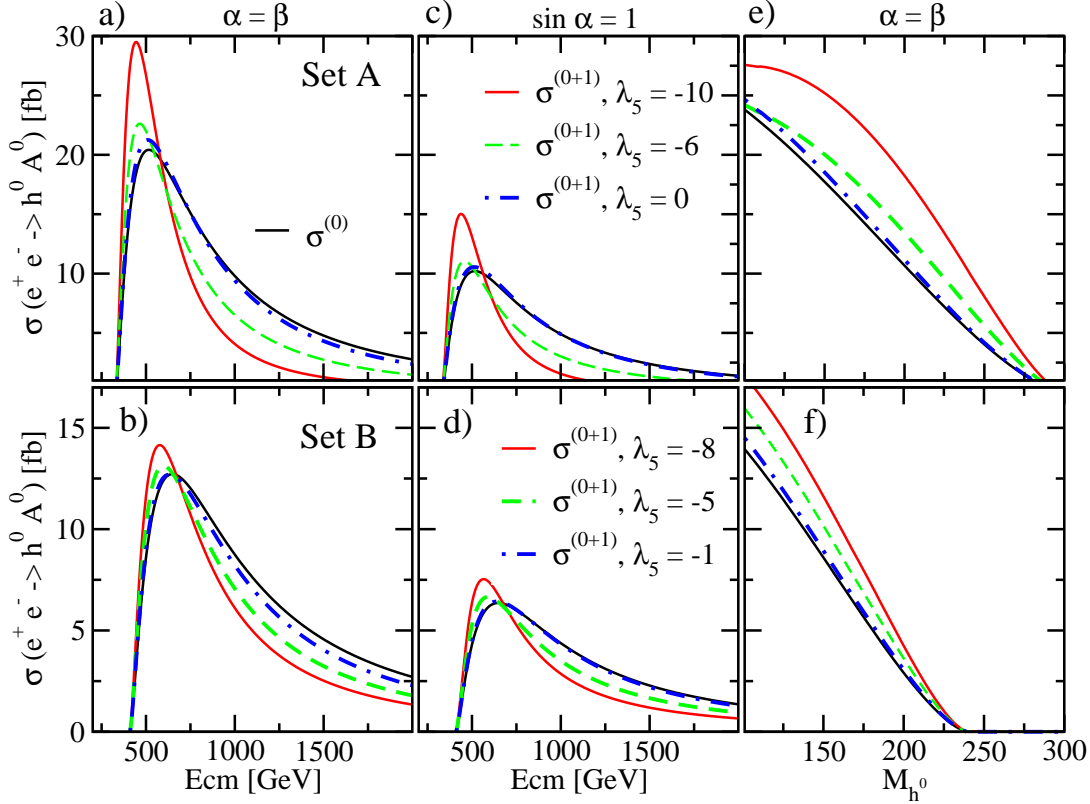


Figure 2: Total cross section $\sigma(e^+e^- \rightarrow A^0 h^0)$ (in fb) at the tree-level and at one-loop for different values of λ_5 and for Sets A (top panels) and B (bottom panels) of Higgs boson masses. Displayed is the behavior of σ as a function of \sqrt{s} (left and center) and M_{h^0} (right panels).

All these trademark phenomenological features become also patent in Figure 2, in which we explore the evolution of the $h^0 A^0$ production cross-section for the following setups: a-b) as a function of \sqrt{s} , for $\alpha = \beta$ (maximum $h^0 A^0 Z^0$ coupling); c-d) the same, for $\alpha = \pi/2$ (the so-called *fermiophobic* limit for the h^0 boson within type-I 2HDM); and e-f) as a function of M_{h^0} , for $\alpha = \beta$. The results are presented for Sets A (upper row) and B (lower row). The phenomenological footprint of 3H self-couplings is easily read off from the dramatic differences in the one-loop production rates when the value of λ_5 is varied in the theoretically allowed range. As for the behavior with M_{h^0} , these plots illustrate a twofold effect on σ ; one is purely kinematical, and accounts for the decrease of the cross-section owing to the reduction of the available phase space; the other is dynamical, and explains why the tree-level cross-sections decouple faster than their corresponding one-loop counterparts; indeed, several 3H self-couplings get boosted with M_{h^0} and can partially counterbalance the phase space suppression.

	0.5TeV	1.0TeV	1.5TeV	0.5TeV	1.0TeV	1.5TeV
	Set A			Set B		
$\sigma(h^0 A^0)$ [fb]	26.71	4.07	1.27	11.63	6.11	2.52
$\sigma(h^0 H^0 A^0)$ [fb]	0.02	5.03	3.55	below thres.	1.25	1.33
$\sigma(H^0 H^+ H^-)$ [fb]	0.17	11.93	8.39	below thres.	0.69	2.14
$\sigma(h^0 h^0 + X)$ [fb]	1.47	17.36	38.01	0.92	9.72	23.40

Table 2: Comparison of the predictions for the cross sections corresponding to several Higgs-pair and triple-Higgs production channels, for Sets A and B of Higgs masses; $\tan\beta = 1$, $\alpha = \beta$, and three different values of the center-of-mass energy. The complementarity between the different channels at different energies becomes manifest here.

4. Discussion and conclusions

We have undertaken a comprehensive study of the neutral 2H production from a generic 2HDM in the context of the ILC/CLIC colliders. The upshot of our analysis spotlights very significant radiative corrections, typically up to $|\delta\sigma/\sigma| \sim 50\%$, which may be either positive (for $\sqrt{s} \simeq 0.5$ TeV) and negative (for $\sqrt{s} \simeq 1$ TeV and above), and basically concentrated in the regions with $\tan\beta \sim 1$ and $|\lambda_5| \sim 10$, with $\lambda_5 < 0$. Such enlarged quantum effects can be basically traced back to the Higgs-mediated 1-loop corrections to the hA^0Z^0 interaction, these being sensitive to potentially enhanced 3H self-couplings – a genuine feature of the 2HDM, with no counterpart in the MSSM. In the most favorable scenarios, the predicted 2H rates furnish a few dozen fb per 500fb^{-1} of integrated luminosity. In practice, these 2H processes would boil down to $A^0 \rightarrow \bar{b}b/\tau^+\tau^-$, and $h^0 \rightarrow \bar{b}b/\tau^+\tau^-$ or $h^0 \rightarrow VV \rightarrow 4l, 2l+$ missing energy, depending on the actual value of M_{h^0} ; all these signatures being feasible in the clean environment of linac facilities. Besides, the analysis of such pairwise Higgs events should be useful to enlighten the inner structure of the underlying Higgs sector, in particular if combined with complementary Higgs production channels such as $e^+e^- \rightarrow hhh$ [3] and $e^+e^- \rightarrow hh + X$ [5]. In Table 2 we quantify the latter statement by plugging $\sigma^{(0+1)}$ for $h^0 A^0$ together with the predicted (leading-order) production rates for several complementary multi-Higgs channels in e^+e^- collisions, assuming maximum 3H self-coupling enhancements (as e.g. Table 1). This pattern of signatures at different \sqrt{s} is highly distinctive of the 2HDM and could not be attributed to e.g. the MSSM, as they critically depend on the 3H self-couplings – which are fully inconspicuous in the latter model owing to supersymmetric invariance. Additional, and very valuable, information can also be obtained from the study of the quantum effects on the production of a neutral 2HDM Higgs boson in association with the Z boson [17].

We conclude that 3H self-couplings may stamp genuine footprints on multi-Higgs production processes, either at leading-order or through quantum corrections, and provide a plethora of complementary signatures whose detection should be perfectly feasible at future linac facilities and, if ever observed, might constitute a strong hint of non-standard, non-supersymmetric Higgs physics.

Acknowledgments This work has been supported in part by the EU project RTN MRTN-CT-2006-035505 Heptools. DLV acknowledges an ESR position of this network and also the support of the MEC FPU grant Ref. AP2006-00357. He also wishes to thank the hospitality of the Theory Group at the Physikalisches Institut of the University of Bonn. JS has been supported in part by MEC and FEDER under project FPA2007-66665, by the Spanish Consolider-Ingenio

2010 program CPAN CSD2007-00042 and by DIUE/CUR Generalitat de Catalunya under project 2009SGR502.

References

- [1] J.F. Gunion, H.E. Haber, G.L. Kane and S. Dawson, *The Higgs hunter's guide*, Addison-Wesley, Menlo-Park, 1990.
- [2] H.P Nilles, Phys. Rept. **110** (1984) 1; H.E. Haber and G.L. Kane, Phys. Rept. **117** (1985) 75; S. Ferrara, ed., *Supersymmetry*, vol. 1-2 (North Holland/World Scientific, Singapore, 1987).
- [3] G. Ferrera, J. Guasch, D. López-Val and J. Solà, Phys. Lett. **B659** (2008) 297; PoS RADCOR2007, 043 (2007), arXiv:0801.3907 [hep-ph].
- [4] A. Arhrib, R. Benbrik and C.-W. Chiang, Phys. Rev. **D77** (2008) 115013.
- [5] R. N. Hodgkinson, D López-Val and J. Solà, Phys. Lett. **B673** (2009) 47.
- [6] N. Bernal, D. López-Val and J. Solà, Phys. Lett. **B677** (2009) 38.
- [7] F. Cornet and W. Hollik, Phys. Lett. **B669** (2008) 58; E. Asakawa, D. Harada, S. Kanemura, Y. Okada and K. Tsumura, Phys. Lett. **B672** (2009) 354; A. Arhrib, R. Benbrik, C.-H. Chen, and R. Santos, Phys. Rev. **D80** (2009) 015010.
- [8] A. Djouadi, H.E. Haber and P.M. Zerwas, Phys. Lett. **B375** (2003) 1996; A. Djouadi, W. Kilian, M. Mühlleitner, and P. M. Zerwas, Eur. Phys. J **C10** (1999) 27, arXiv:hep-ph/9903229
- [9] P. Chankowski, S. Pokorski and J. Rosiek, Nucl. Phys. **B423** (1994) 437; V. Driesen and W. Hollik, Zeitsch. f. Physik **C68** (1995) 485; V. Driesen, W. Hollik and J. Rosiek, Zeitsch. f. Physik **C71** (1996) 259; S. Heinemeyer, W. Hollik, J. Rosiek and G. Weiglein, Int. J. of Mod. Phys. **19** (2001) 535; A. Arhrib and G. Moutaka, Nucl. Phys. **B558** (1999) 3; E. Coniavitis and A. Ferrari, Phys. Rev. **D75** (2007) 015004.
- [10] J. Guasch, W. Hollik and A. Kraft, Nucl. Phys. **B558** (1999) 3.
- [11] D. López-Val and J. Solà, arXiv:0908.2898 [hep-ph]; accepted in Phys. Rev. D.
- [12] see e.g. S. Kanemura, T. Kubota and E. Takasugi, Phys. Lett. **B313** (1993) 155; A.Arhrib, arXiv:hep-ph/0012353.
- [13] C. Amsler et al. (Particle Data Group), Phys. Lett. **B667** (2008) 1
- [14] M. Misiak and M. Steinhauser, Nucl. Phys. **B764** (2007) 62; M. Misiak et al., Phys. Rev. Lett. **98** (2007) 022002.
- [15] M. Bohm, H. Spiesberger and W. Hollik, *Fortsch. Phys.* **G34** (1986) 87; A. Denner, *Fortsch. Phys.* **G41** (1993) 307.
- [16] T. Hahn, *FeynArts 3.2, FormCalc and LoopTools*, <http://www.feynarts.de>; T. Hahn, *Comput. Phys. Commun.* **168** (2005) 78.
- [17] N. Bernal, D. López-Val and J. Solà (in preparation).